Journal of Neurochemistry, 2007, **103**, 2224–2233 doi:10.1111/j.1471-4159.2007.04917.x

Visible light induces matrix metalloproteinase-9 expression in rat eye

Andrea M. Papp,* Rita Nyilas,* Zsuzsanna Szepesi,* Magor L. Lőrincz,* Eszter Takács,* István Ábrahám,* Nóra Szilágyi,† Júlia Tóth,‡ Péter Medveczky,‡ László Szilágyi,‡ Gábor Juhász§ and Gábor Juhász*

**Laboratory of Proteomics, Institute of Biology, Eötvös Loránd University, Budapest, Hungary*
†*Department of Physiology and Neurobiology, Eötvös Loránd University, Budapest, Hungary*
‡*Department of Biochemistry, Eötvös Loránd University, Budapest, Hungary*
§*Department of Anatomy, Cell and Developmental Biology, Eötvös Loránd University, Budapest, Hungary*

Abstract

Up-regulation of matrix metalloproteinase-9 (MMP-9, gelatinase B) in the nervous system has been demonstrated when excitotoxicity-induced tissue remodeling and neuronal death occurs. Induction of MMP-9 by a natural stimulus has not been observed yet. Using RT-PCR and gelatin-zymography we demonstrated MMP-9 induction at transcriptional and protein levels in different structures of the rat eye following over-stimulation with white light. MMP-9 elevation occurred in the retina without reduction in photoreceptor number or major anatomical reorganization. A transient decrease in electroretinogram b-wave indicated the functional recovery. Retrobulbar injection of a broad-spectrum MMP-inhibitor GM6001, slowed the recovery rate of b-wave amplitude. Even room-light applied to dark-adapted awake animals induced MMP-9 increase in the retina, which suggests a role for MMP-9 in physiological functional plasticity of the nervous system, such as light adaptation. This is the first demonstration of MMP-9 induction by a sensory stimulus.

Keywords: b-wave, electroretinogram, gelatinase B, GM6001, light, matrix metalloproteinase-9.
J. Neurochem. (2007) **103**, 2224–2233.

Matrix metalloproteinase-9 (EC 3.4.24.35, Gelatinase B, MMP-9) is an inducible member of MMP family (Van den Steen *et al.* 2002) with established role in the CNS in tissue remodeling and cell death triggering (Gu *et al.* 2002; Rivera *et al.* 2002; Jourquin *et al.* 2003; Lee *et al.* 2004). MMP-9 induction in the CNS has been demonstrated in different excitotoxic paradigms like kainate model of epilepsy (Zhang *et al.* 1998; Szklarczyk *et al.* 2002; Jourquin *et al.* 2003) and ischemia (Rosenberg *et al.* 1996; Planas *et al.* 2001). Recently, MMP-9 induction was found in nervous tissue-specific plasticity processes like sleep deprivation (Taishi *et al.* 2001), spatial memory formation (Wright *et al.* 2003; Meighan *et al.* 2006), and hippocampus-dependent associative learning (Nagy *et al.* 2006). Thus, a more general contribution of MMP-9 to the modulation of information transmission in the nervous system emerges. In this context, we aimed to determine the putative induction and/or activation of MMP-9 by sensory stimuli leading to adaptation or by high-intensity stimuli triggering functional disturbances.

The light-exposed retina is a good model with its network of neuronal and glial components of central origin. Depending on intensity, light can induce physiological as well as pathological processes in the retina, especially in its outer nuclear layer (ONL) (Noell *et al.* 1966; Malik *et al.* 1986; Young 1994), and light-history can influence susceptibility of photoreceptors to light-damage (Penn *et al.* 1987; Stone *et al.* 1999). Therefore, MMP-induction in the retina can be studied by adjusting light intensity from physiological to pathological range.

Expression of MMP-9 has been demonstrated in several ophthalmologic diseases in different eye structures (Abu El-Asrar *et al.* 1998; Salzmann *et al.* 2000; Wong *et al.* 2002; Zhang and Chintala 2004). However, the exact cellular origin of MMP-9 is uncertain in most of these diseases (Sivak and Fini 2002). In the retina, induction of MMP-9 was observed in ischemia-reperfusion (Zhang *et al.* 2002) and kainate-induced excitotoxicity (Zhang *et al.* 2004), but MMP-9 induction without tissue damage in the eye is yet unevaluated.

Received May 7, 2007; revised manuscript received July 25, 2007; accepted August 7, 2007.

Address correspondence and reprint requests to Gábor Juhász, Laboratory of Proteomics, Institute of Biology, Eötvös Loránd University, H-1117 Budapest, Pázmány P. stny. 1/C., Hungary.
E-mail: gjuhasz@dec001.geobio.elte.hu

Abbreviations used: DMSO, dimethyl sulfoxide; ERG, electroretinogram; LED, light-emitting diode; MMP, matrix metalloproteinase; ONL, outer nuclear layer; RPE, retinal pigment epithelium; TBST, Tris-buffered saline-Tween; TUNEL, terminal deoxynucleotidyl transferase-mediated tetramethylrhodamine-dUTP nick end-labeling.

Role of MMP-9 in wound healing in the eyeball was already revealed (Fini *et al.* 1992), but there is no data about contribution of MMP-9 to the functional recovery of the retina.

Retinal function can be monitored by recording the electroretinogram (ERG) as reduction of its b-wave amplitude correlates with retinal damage (Sugawara *et al.* 2000). Relying on our recently developed method, ERG can be recorded from freely moving rats (Galambos *et al.* 2000; Szabó-Salfay *et al.* 2001) and the induction of MMP-9 in the retina could be correlated with long-term changes in visual function.

We found that MMP-9 induction occurs in the retina at different light-intensities. After photo-stress, retinal function recovered as shown by ERG b-wave and this recovery was attenuated by an MMP-inhibitor. Our findings suggest that MMP-9 is an inducible dynamic protease contributing to adaptation, functional recovery, and/or protection of the retina.

Materials and methods

Animals and reagents

Experiments were carried out on 350–400 g male Sprague–Dawley rats (Charles River Laboratories, Budapest, Hungary), reared under 12 h light (500 lux) : 12 h dark cycles. Animals were kept and the experiments were performed in conformity with the Council Directive 86/609/EEC, the Hungarian Act of Animal Care and Experimentation (1998, XXVIII) and local regulations for care and use of animals for research. All reagents were from Sigma-Aldrich Co. (St Louis, MO, USA), unless otherwise stated.

Experimental paradigms

Photo-stress model

Following overnight dark adaptation (less than 0.17 lux), rats were anesthetized intramuscularly with a mixture of ketamine (80 mg/kg, Novartis, Budapest, Hungary) and xylazine (8 mg/kg, 2% Primazin; Alfasan, Woerden, Nederland), and placed in a stereotaxic frame (David Kopf Instruments, Tujunga, CA, USA). Mydriasis was induced bilaterally by 2.5% phenylephrine hydrochloride (SCHEIN Pharmaceutical Inc., Florham, NJ, USA). Each eye was exposed for 3 h to 5500 lux white light delivered by two light-emitting diodes [LEDs (XWA-L50 ACA-B4, 5 mm outer diameter, 6000 mcd; Lite-On, Taipei, Taiwan] placed at 1 mm from the corneal surfaces. The light-spectra of LEDs ranged from 400 to 650 nm (peak emission at 440 and 525 nm). There was no UV emission and the surface temperature of LEDs remained below 38°C during experiments. Eyes were enucleated at 0, 3, 6, 12 h, and 1, 2, 3, 7, and 10 days after the end of light exposure. Animals were kept in darkness during their individual survival period.

Effect of xylazine

All animals were dark-adapted overnight. A ketamine–xylazine anesthetized, photo-stress exposed group was compared to the following controls (two rats/group): (i) rats dark-adapted for further 9 h without anesthesia, (ii) ketamine–xylazine anesthetized rats kept in darkness for 9 h, and (iii) photo-stress subjected rats anesthetized by ketamine only. Samples for zymography were collected 6 h after photo-stress and 9 h after the beginning of the experiment for controls not exposed to photo-stress.

Retrobulbar injection of matrix metalloproteinase-inhibitor

Three anesthetized rats received unilateral retrobulbar injection of 75 μL GM6001 (1 mg/mL, Ilomastat; Chemicon International Inc., Temecula, CA, USA) 30 min before photo-stress. The broad-spectrum MMP-inhibitor GM6001 being delivered as a dimethyl sulfoxide (DMSO) stock solution, retrobulbar injection of 75 μL of DMSO was used as control in the contralateral eye. Drugs were delivered by slow injection into the retrobulbar space.

Room-light re-exposure

In light adaptation studies, zymograms of three experimental groups (four rats/group) were compared: (i) rats exposed to normal rearing light conditions (12 h : 12 h light : dark cycles, 500 lux), (ii) controls dark-adapted for 11 days, and (iii) 10-days dark-adapted animals subjected to 500 lux natural light for 12 h. In light exposed rats, eyes were removed at the end of a 12-h dark period.

Electroretinogram

A corneal electrode and a retrobulbar stimulating red LED were implanted unilaterally (photo-stress only) or bilaterally (GM6001 injected), along with a reference electrode, in halothane anesthesia (1% in air; Leciva, Praha, Czech Republic), as described earlier (Szabó-Salfay *et al.* 2001). Briefly, a non-pyrogenic corneal electrode of teflon-coated stainless steel multistrand wire (Medwire 7SST1; Sigmund Cohn Corp., Mount Vernon, NY, USA) was placed under the upper eyelid in contact with the corneal surface. The retrobulbar stimulating red-LED of 5 mm outer diameter, with transparent body (3000 lux/mm^2; Bright LED Electronics, Hong Kong) was fixed to the skull with its light-beam oriented towards the posterior pole of the eyeball. This position of the LED allows delivery of constant light-flashes to the retina, the number of photons reaching the photoreceptors being independent of head- and eyelid-positions and of pupil-diameter. A reference electrode of 4×8 mm stainless steel plate insulated on one side was introduced under the skin over the left masseter muscle. Electrode- and stimulating LED-wires were soldered to separate plugs fixed to the skull with dental cement.

After 7-day recovery, five rats were exposed to photo-stress and three received a unilateral retrobulbar injection of GM6001 and of DMSO in the contralateral eye 30 min before photo-stress. ERG was evoked by 1 ms flashes delivered by a digitally controlled stimulator (Biostim; Supertech Ltd., Pécs, Hungary). The inter-stimulus interval was 10 s, allowing retinal recovery. A Grass B8 EEG (Grass Technologies, West Warwick, RI, USA) machine using 1 Hz–10 kHz band-pass and 10 K gain recorded the evoked responses. Data acquisition was performed by CED 1401 digital data capture system (Cambridge Electronic Design Ltd., Cambridge, UK; 500 Hz sampling rate, 1000 ms frame-length). Signal 1.906 software (Cambridge Electronic Design) averaged ERGs (70 sweeps/average) from anesthetized rats during photo-stress and from dark-adapted freely moving rats at all time-points afterwards. In GM6001-injected rats, after 20 min dark adaptation following photo-stress, the ERG was recorded continuously from

both eyes for 330 min and averaged at 10 min intervals. Peak-to-peak amplitudes of ERG b-wave were measured.

Morphology

Eyes were enucleated under ketamine–xylazine anesthesia; embedded into Tissue-Tek OCT (Sakura Finetek Co., Tokyo, Japan); frozen in liquid nitrogen and stored at −70°C. Sagittal cryosections of 10 μm were stained with hematoxylin-eosin. Retinas of 10-day dark-adapted controls and of photo-stress exposed rats, recovered for 10 days in darkness (n = 4/group) were compared. A BX51 microscope (Olympus, Budapest, Hungary) was used for qualitative evaluation of sections, and the images were captured with Analysis Pro 3.2 software (Soft Imaging System GmbH, Münster, Germany). Two sagittal sections of the ONL at the level of the optic nerve head were examined from both eyes per animal. The number of cell nuclei was counted in a 150 × 80 μm area from corresponding parts of the retina at 60× magnification.

Terminal deoxynucleotidyl transferase-mediated tetramethylrhodamine-dUTP nick end-labeling

For *in situ* DNA fragmentation analysis by terminal deoxynucleotidyl transferase-mediated tetramethylrhodamine-dUTP nick end-labeling (TUNEL)-method retina sections from two experimental groups were compared (n = 4/group): photo-stress exposed rats allowed a 20-h survival period in darkness and a control group returned for 23 h to dark immediately after anesthesia. Eyes were enucleated, fixed overnight in 3.7% (wt/vol) formaldehyde in phosphate-buffered saline (pH 7.6) at 4°C, and embedded in paraffin. Twenty-micrometer sagittal sections from dark-adapted control retinas treated with 20 U/mL DNase I served as positive staining-control. TUNEL-staining was performed with tetramethylrhodamine red *in situ* cell death detection kit (Roche Diagnostics GmbH, Mannheim, Germany) according to the manufacturer's recommendations. DNA was stained with Sytox Green (Invitrogen Ltd., Paisley, UK) in all sections. An Olympus IX81 confocal microscope was used to capture images with identical settings across parallel samples. Image acquisition was performed with Fluoview 500 software (Olympus) and ten 1-μm optical sections/image were finally overlaid.

Eye dissection

After experimental light exposure, rats were kept in dark. Eyes were enucleated in ketamine–xylazine anesthesia, and dissected on ice into cornea, vitreous, retina, and sclera samples. The 'sclera' sample contained the retinal pigment epithelium (RPE) and choroid too. For zymography, samples were homogenized immediately in 10 mmol/L $CaCl_2$ and 0.25% (vol/vol) Triton X-100 solution (20 μL/mg wet tissue). For total RNA isolation, samples were frozen in liquid nitrogen and stored at −70°C.

Matrix metalloproteinase gelatin zymography

Tissue homogenates for gelatin zymography were prepared based on the procedure of Weeks *et al.* (1976) and Szklarczyk *et al.* (2002), with slight modifications. Briefly, after initial homogenization, samples (n = 3/each time point/structure) were centrifuged at 6000 *g* for 20 min at 4°C. The supernatant (Triton X-100 soluble fraction containing the intracellular and cell membrane bound MMPs) and the pellet (Triton X-100 insoluble fraction containing the extracellular matrix bound fraction of MMPs) were processed separately. The supernatant was precipitated with cold ethanol (final concentration 60%) for 5 min on ice. Following centrifugation at 15 000 *g* for 5 min at 4°C, the precipitate was resuspended in non-reducing sodium dodecyl sulfate (SDS)-buffer (125 mmol/L Tris–HCl pH 6.5, 2% (wt/vol) SDS, 20% (vol/vol) glycerol, 0.01% (wt/vol) bromphenol blue; 5.3 μL/1 mg initial wet tissue), then incubated for 15 min at 37°C with repeated vortexing. The Triton X-insoluble pellet was resuspended in an equal volume of buffer [50 mmol/L Tris–HCl (pH 7.4), 0.1 mol/L $CaCl_2$, 20 μL/mg of initial wet tissue] and incubated for 15 min at 60°C. Centrifugation at 10 000 *g* for 20 min at 4°C was followed by quantitative removal of the supernatant, which was then processed similarly to the Triton X-soluble fraction, and finally solubilized in SDS-buffer (2.7 μL/1 mg initial wet tissue). Total protein content was determined with bicinchoninic acid protein assay kit. Equal amounts of proteins along with pre-stained molecular weight standards (MBI Fermentas Inc., Hanover, MD, USA) were separated by SDS-polyacrylamide gel electrophoresis under non-reducing conditions using 7.5% polyacrylamide gels copolymerized with 0.1% FITC-labeled gelatin. This method allows real-time monitoring of enzymatic activity under UV light and shows higher sensitivity as compared to Coomassie staining. It has to be noted that differently from Coomassie stained gels, in fluorescent-zymography gelatinolysis is detected as dark bands against a bright fluorescent background (Hattori *et al.* 2002). Gels were washed twice for 15 min each in 100 mL of 2.5% (vol/vol) Triton X-100 to remove SDS then incubated for 48 h at 37°C in 100 mL buffer containing 50 mmol/L Tris–HCl (pH 7.5), 10 mmol/L $CaCl_2$, 1 μmol/L $ZnCl_2$, 1% (vol/vol) Triton X-100, 0.02% (wt/vol) NaN_3. After this in-gel MMP-renaturation (Szklarczyk *et al.* 2002), zymograms were digitized with Geldoc1000 gel documentation system (Bio-Rad Laboratories Inc., Hercules, CA, USA) in UV light.

To validate the MMP origin of gelatinolytic bands, samples were incubated for 48 h at 37°C in assay buffer supplemented with one of the following proteinase inhibitors: 0.5 mmol/L 1,10-phenantroline; 10 mmol/L EDTA; 2 mmol/L phenylmethanesulfonyl fluoride; 2.5 μg/mL aprotinin; 1 mmol/L leupeptine; or 1 μg/mL pepstatine. Phenantroline and EDTA inhibited the gelatinolytic activity, while the other proteinase inhibitors had no effect (data not shown).

Western blot detection of matrix metalloproteinase-2 and matrix metalloproteinase-9

For western blot analysis, samples were resuspended in SDS-buffer supplemented with 10% (vol/vol) β-mercaptoethanol. Protein bands were electrically transferred to nitrocellulose membranes (Bio-Rad Laboratories Inc.). The membranes were blocked for 1 h at 23°C in Tris-buffered saline-Tween (TBST) [20 mmol/L Tris–HCl pH 7.6, 132.5 mmol/L NaCl, 0.05% (vol/vol) Tween-20] containing 5% (wt/vol) non-fat milk, then incubated overnight at 4°C with purified rabbit antibodies against MMP-2 or MMP-9 (TP-220, TP-221; Torrey Pines Biolabs Inc., Houston, TX, USA) at 1 : 2000 dilution in TBST. After incubation for 1 h at 23°C with horseradish peroxidase-conjugated polyclonal goat anti-rabbit antibody (Dako Cytomation, Copenhagen, Denmark; dilution 1 : 2000 in blocking buffer), the MMPs were visualized on X-ray films using Supersignal West Pico Chemiluminescent Substrate (Pierce, Rockford, IL,

USA). Between all incubation steps, the membranes were washed extensively with TBST.

Total RNA isolation and RT-PCR

Tri Reagent (Molecular Research Center Inc., Cincinnati, OH, USA) was used for total RNA isolation following the manufacturer's protocol (1995). The purity of each sample (A260/A280 between 1.6 and 1.9) and total RNA concentration were evaluated spectrophotometrically (40 μg RNA/mL per one unit of absorbance at 260 nm). Isolated total RNA was stored at −70°C until further use. Reverse transcription was performed with random hexamer primers and 3 μg of total RNA as template using revertaid first strand cDNA synthesis kit (MBI Fermentas Inc.). Starting with 3 μL cDNA, PCR reactions were performed for 40 cycles at optimized annealing temperatures (52°C for MMP-2; 54°C for MMP-9 and β-actin), using the following forward and reverse primers (synthesized by Genodia Ltd., Budapest, Hungary): 5′-CTATTCTGTCAGCACTTTGG-3′ and 5′-CAGACTTTGGTTCTCCAACTT-3′ for MMP-2 and 5′-AAATGTGGGTGTACACAGGC-3′ and 5′-TTCACCCGGTTGTGGAAACT-3′ for MMP-9, respectively. For loading control β-actin primers were used (forward primer 5′-TCCTTCCTGGGTATGGAATC-3′; reverse primer 5′-ACTCATCGTACTCCTGCTTG-3′). The amplified product lengths were 300, 309, and 309 bp, respectively. Three (β-actin) and 5 μL (MMP-2, MMP-9) of the amplification products were subjected to electrophoresis on 0.5% ethidium bromide containing 2% agarose gel in Tris borate-EDTA buffer. Bands were visualized with a UV-transilluminator. Digital images were recorded with Geldoc1000 (Bio-Rad Laboratories Inc.) and densitometry was performed using Uvisoft Gel Analysis v.10.02 software (Uvitec Ltd., Cambridge, UK). Initially, the time course of MMP-9 mRNA levels was determined separately for each eye structure. Data were averaged in the period of maximal MMP-9 induction: retina (0–24 h), vitreous body (24–72 h), sclera (12–72 h), and cornea (6–72 h). MMP-2 mRNA levels of the same timeframes were averaged.

Data processing and statistical analysis

All graphics and statistics on electrophysiology and densitometry data were performed using Origin 7.0 software (OriginLab Corporation, Northampton, MA, USA). Independent Student *t*-test was applied to compare changes in different groups. For statistical analysis of the quantitative histology results, non-parametric Mann–Whitney *U*-test of Statistica v. 5 (Statsoft Inc., Tulsa, OK, USA) was used. Statistical significance was considered at $p < 0.05$. Comparison of b-wave amplitude recovery rate in control- versus GM6001-injected rats was based on the first and second derivative of ERG b-wave amplitude-recovery time function as follows. First, the recovery time-series data were fitted by second order (quadratic) polynomials (recovery curves) to determine exactly the recovery rates. Then, the rate itself was quantified by the first order derivative of the recovery curve. Since the derivative is a linear function of recovery time, its two parameters (slope and intercept) were used to measure the MMP-inhibitor effect compared to control condition. Polynomial fitting and slope analysis were calculated in Matlab software environment (The MathWorks Inc., Natick, MA, USA) by self-devised scripts.

Results

Functional recovery of electroretinogram and outer nuclear layer morphology after photo-stress

During the 3-h exposure to white light of 5500 lux the ERG was transiently abolished (to 0.16 ± 0.1%), but started to recover progressively as the photo-stress ended. The b-wave amplitude reached 32.8 ± 7.9% of the control value after 3 h in darkness. The gradual increase continued up to 24 h, when it reached 89.1 ± 13.4%. After 24 h, b-wave amplitude stabilized at ∼83–89% of control values, which was not significantly different from the control (Fig. 1a and b).

The functional recovery of the retina, as revealed by ERG, was accompanied with lack of morphological changes as shown by hematoxylin-eosin staining (Fig. 1c). Quantitative histological analysis of sagittal sections through the optic nerve head did not reveal significant (non-parametric Mann–Whitney *U*-test, $p < 0.05$) cell number difference in ONL between 10-days dark-adapted controls ($N = 352.3$; SD: 31.8, $n = 4$) and bright light-exposed animals survived 10 days in darkness ($N = 310.6$; SD: 36.3, $n = 4$). Further-

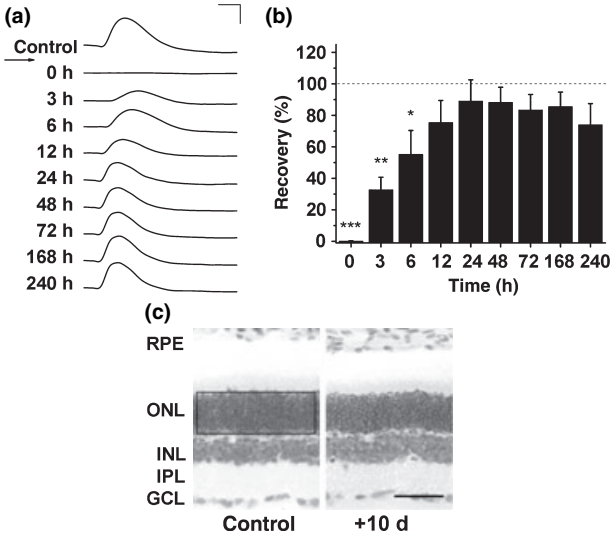

Fig. 1 Photo-stress (5500 lux for 3 h) causes reversible functional disturbances without detectable reduction in the number of photoreceptor cells or major anatomical reorganization in the retina. (a) Representative ERGs registered before and after light exposure (0 h, ERG at the end of photo-stress, shown by arrow; scale bars, 50 ms and 50 μV; 40 points Fast Fourier transform smoothing). (b) Histogram of b-wave amplitudes, as % of control values, at different time-points after photo-stress (mean ± SEM, $^*p < 0.05$, $^{**}p < 0.01$, $^{***}p < 0.001$). (c) Hematoxylin-eosin stained sections of the retina: 10-day dark-adapted control (control) compared to rat kept 10 days in dark after photo-stress (+10 d). RPE, retinal pigment epithelium; ONL, outer nuclear layer; INL, inner nuclear layer; IPL, inner plexiform layer; GCL, ganglion cell layer; scale bar, 50 μm; rectangle shows the 150 × 80 μm area used for counting photoreceptor nuclei.

more, *in situ* DNA fragmentation analysis by TUNEL-method showed that the staining in ONL at 20-h post-photostress was negligible compared to DNase-treated sections, similarly to dark-adapted control retinas (Fig. 2).

Matrix metalloproteinase-9 and matrix metalloproteinase-2 protein and mRNA changes after photo-stress

On zymograms of control retinal samples, MMP-2 (65–72 kDa) was present, while pro-MMP-9 (~92–100 kDa) was hardly detectable. The gelatinolytic band of pro-MMP-9 became detectable from 3 h after light exposure, peaked at 6 h and returned to undetectable levels at 72 h (Fig. 3a). In vitreous body and sclera samples, pro-MMP-9 induction was detected at 3 h, reached maximum at 6–12 h and returned to baseline level after 48 and 168 h, respectively (Fig. 3b and c). Changes of pro-MMP-9 in the cornea showed a similar pattern to sclera samples (Fig. 3d). We observed only minor differences in the kinetics of MMP-9 induction between gelatin zymograms of soluble and insoluble fractions in all tissue compartments of the eye (Fig. 3a–d). The majority of MMP-2 activity was found in the Triton X-100 soluble fractions and photo-stress increased the gelatinolytic activity in each eye structure studied (Fig. 3a–d), especially in the sclera (Fig. 3c).

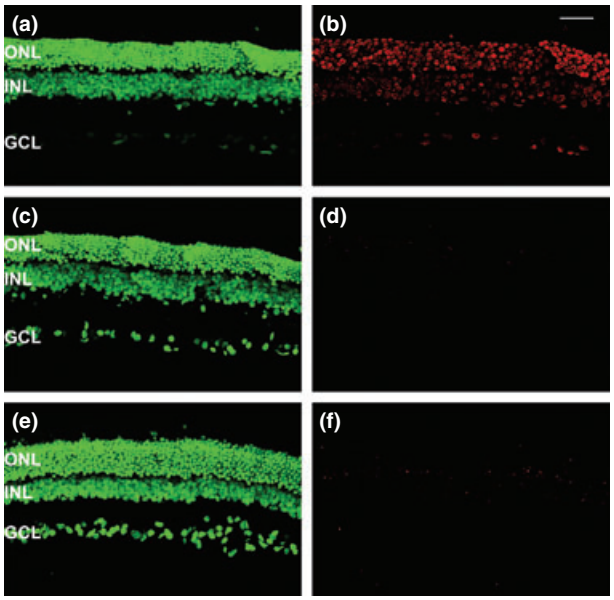

Fig. 2 *In situ* analysis of DNA fragmentation in retina sections. (a, c, e) Sytox Green DNA staining; (b, d, f) TMR-labeled TUNEL-staining. (a, b) DNase-treated (20 U/mL) section from dark-adapted control retina, as positive staining control; (b, c) Dark-adapted control retina; (d, e) Photo-stress exposed retina after 20 h survival period in darkness (scale bar, 40 μm; ONL, outer nuclear layer; INL, inner nuclear layer; GCL, ganglion cell layer).

Western blot analysis confirmed the MMP-9 origin of the 92–100 kDa gelatinolytic band. In addition, a positive reaction at ~65 kDa was detected (Fig. 4c). The 72-kDa band was verified by MMP-2 antibody (Fig. 4c).

As of MMP-9 and MMP-2 mRNA levels are concerned, the elevation of MMP-9 had different time-courses in different eye-structures, while MMP-2 was rather stable in the timeframe corresponding to the maximal induction of MMP-9 in each structure. MMP-2 mRNA increased significantly only in sclera samples (Fig. 3g). In the retina, significant induction of MMP-9 mRNA took place within 24 h following photo-stress (Fig. 3e). Elevation of MMP-9 mRNA occurred also in the sclera and cornea, and lasted for 72 h (Fig. 3g and h, respectively). We note here that MMP-9 mRNA elevation started in the retina, was detected then in cornea, and finally in the sclera and vitreous suggesting a pivotal role for the retina in MMP-9 induction.

Effect of xylazine

Because photo-stress was performed under anesthesia, it was important to determine the effect of the α_2-adrenergic agonist xylazine on MMP induction. MMP-9 and MMP-2 levels were estimated by zymography. Ketamine–xylazine anesthesia increased pro-MMP-9 (~92–100 kDa) level in all samples compared to un-anesthetized, dark-adapted controls. Six hours after bright light exposure similarly elevated pro-MMP-9 in retina, sclera, and vitreous were detected in ketamine–xylazine anesthetized rats and in rats anesthetized without xylazine. In the cornea, however, the elevation of pro-MMP-9 in the light-exposed group receiving xylazine was more pronounced than in the light-exposed animals anesthetized without xylazine. It suggests an MMP-9 inducing effect of xylazine itself in the cornea. MMP-2 (~65–72 kDa) showed significant change only in the sclera 6 h after photo-stress (data not shown).

Effect of matrix metalloproteinase-inhibition on electroretinogram b-wave changes following photo-stress

First, we verified whether GM6001 injected into the retrobulbar space reaches the retina. As it is shown by zymography (Fig 5a), pro-MMP-9, and to a lesser extent, MMP-2 levels decreased by GM6001 in both Triton X-soluble and -insoluble fractions as compared to the sham-injected eye, in retinal samples collected 12 h after photo-stress, supporting that GM6001 reached the retina.

The recovery curves of ERG b-wave amplitudes recorded from DMSO-injected eyes (control group), showed curvilinear pattern and reached saturation at full recovery within 5–5.3 h (Fig. 5b). Applying DMSO + MMP inhibitor GM6001 (treatment group), the recovery of the retinogram b-wave was slower and followed a linear recovery curve. Therefore, the total b-wave recovery in GM6001 treated rats was not reached during 5.3 h (Fig. 5b). As for the b-wave recovery rates (Fig. 5c), in the control group the recovery starts from a

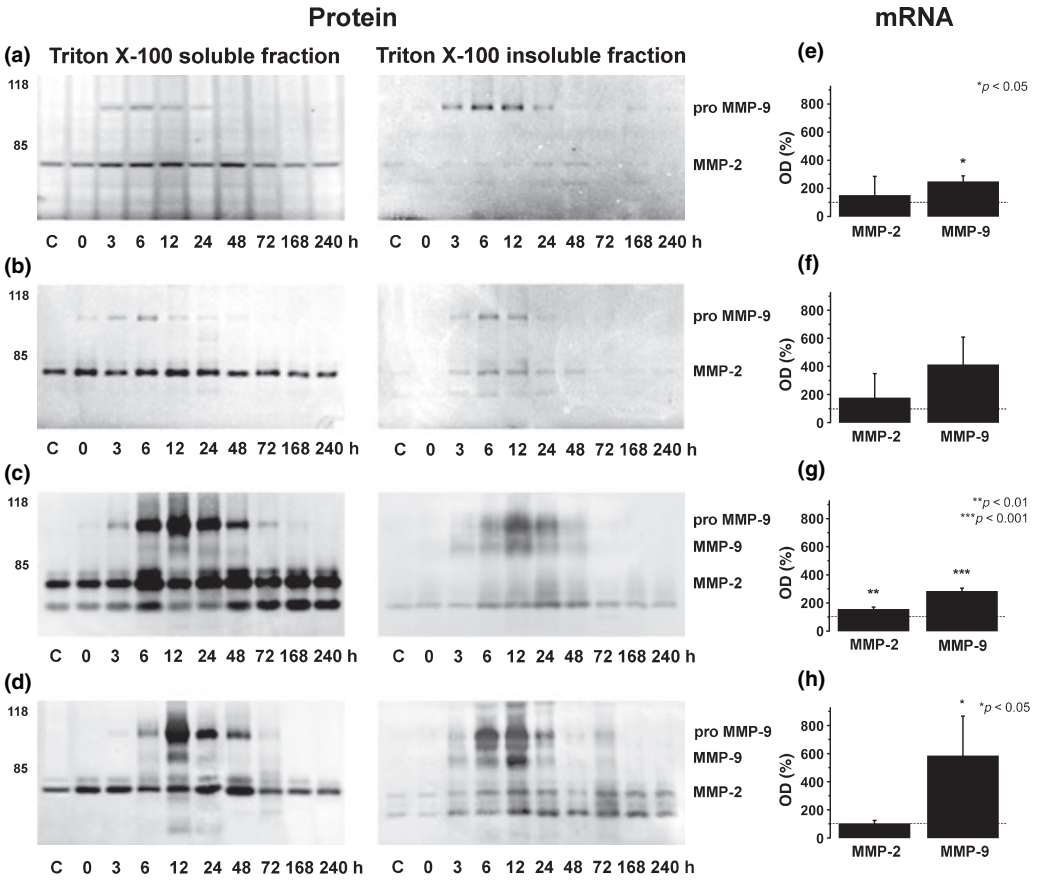

Fig. 3 Spatiotemporal induction of MMP-9 and MMP-2 at protein and mRNA in the rat eye after photo-stress (5500 lux, 3 h). (a–d) Gelatin-zymography of eye samples collected at different time-points (0, 3, 6, 12, 24, 48, 72, 168, and 240 h) after photo-stress and dissected into (a) retina, (b) vitreous body, (c) sclera, and (d) cornea. ('C' represents dark-adapted control samples, from the corresponding eye structure. Numbers at the left side of the zymograms indicate protein weight standards in kDa). (e–h) Changes of MMP-9 and MMP-2 mRNA expression after photo-stress in the (e) retina, (f) vitreous body, (g) sclera, and (h) cornea. *y*-Values represent optical density of RT-PCR amplification products at the peak of the induction of MMP-9 mRNA in % of the control (mean ± SD).

high initial value (high intercept) then undergoes a large-scale deceleration (steep slope) reaching final, near-zero speed. In the treatment group the effect of the inhibitor results in a near-zero initial recovery rate value (low intercept) which remains at these low values during experiment (shallow slope). Since the slope can be interpreted as acceleration of the recovery, while the intercept as the initial speed, we could conclude that the inhibition of MMPs slows the dynamics of the functional recovery process from its beginning.

Adaptation to 500-lux room-light

After long-lasting dark adaptation (10 days) 12 h exposure to room-light conditions (500 lux) resulted in pro-MMP-9 induction only in the retina, in the Triton-insoluble fraction exclusively, as shown by zymography (Fig. 4b). Induction of pro-MMP-9 was not detectable in the sclera, cornea, or vitreous samples, while MMP-2 remained unchanged in all samples (Fig. 4a and b).

Discussion

Retina, embryologically originating from diencephalon is frequently used as a model of CNS because of its easily approachable extracranial localization. However, there are major differences between retina and brain. While in the brain depolarization, action potential generation and glutamate release convey the excitation, in the retina only the ganglion cell layer responds to light with depolarization and action potential generation. The major group of retinal neurons, the photoreceptors, releases glutamate continuously during darkness, while excitation by light triggers their hyperpolarization and decreased glutamate release. In this context, the induction of MMP-9 by light in the retina cannot be directly linked to depolarization and increased glutamate levels as formerly proposed based on glutaminergic excitotoxicity models (Zhang *et al.* 1998; Szklarczyk *et al.* 2002; Gursoy-Ozdemir *et al.* 2004; Mali *et al.* 2005; Manabe *et al.* 2005).

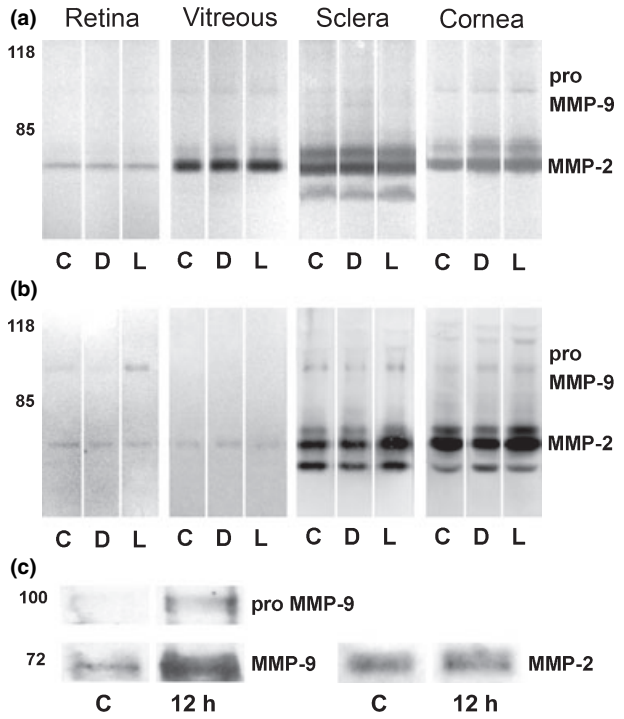

Fig. 4 (a and b) Room-light (500 lux) causes MMP-9-induction in the retina of non-anesthetized, freely moving rats. Gelatin zymography of (a) Triton X-100 soluble and (b) Triton X-100 insoluble fractions of retina, vitreous, sclera, and cornea samples [C, control rat exposed to rearing light conditions (12 h : 12 h light : dark cycle, 500 lux); D, rat kept in darkness for 11 days; L, 10 days dark-adapted animal exposed to 500 lux natural light for 12 h; survival time, 12 h in dark]. (c) Western blot validation of gelatinolytic bands. In Triton X-100 insoluble retinal samples collected 12 h after photo-stress (5500 lux, 3 h) the MMP-9 antibody reacted with the ~92/100 and ~68 kDa bands, while the MMP-2 antibody reacted with the 72-kDa band (C, control; 12 h, 12 h after photo-stress).

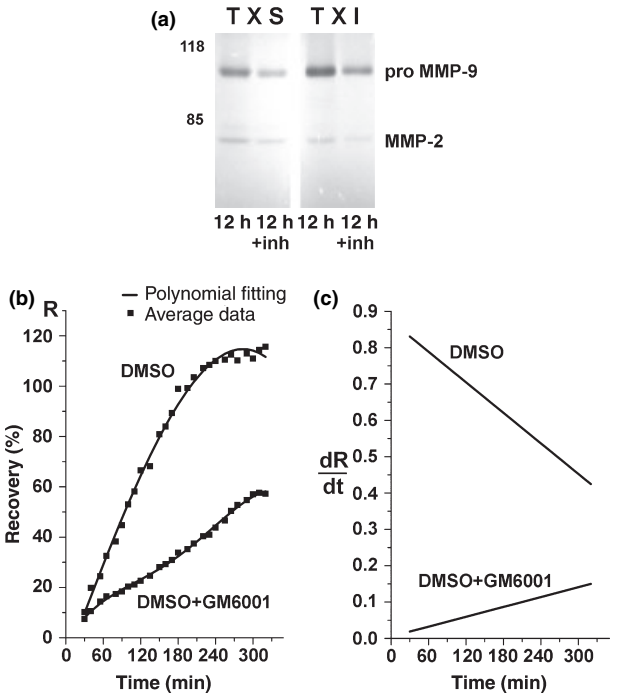

Fig. 5 Effect of the broad-spectrum MMP-inhibitor GM6001 injected retrobulbarly 30 min before photo-stress on retinal changes elicited by photo-stress (5500 lux, 3 h). (a) Partial inhibition of gelatinolytic activity in the retina samples collected 12 h after photo-stress from GM6001 injected eye as compared to the vehicle injected contralateral eye, in Triton X-100 soluble (TX S) and insoluble (TX I) fractions of retina (12 h : 12 h after photo-stress following DMSO injection; 12 h + Inh : 12 h after photo-stress following GM6001 + DMSO injection). (b) Comparison of polynomials fitted to the averaged ERG b-wave amplitudes recorded up to 5.3 h after exposure to photo-stress from vehicle (DMSO) versus MMP-inhibitor (GM6001 + DMSO) injected rat eyes. (c) Comparison of recovery rates, the first order derivatives of the recovery curves shown in (b) (intercept 0.873; slope −0.0014 for DMSO-control; intercept 0.136; slope 0.0001 for GM6001-treated rats).

The use of glutamate receptor antagonist ketamine and α_2-adrenergic agonist xylazine as anesthetic, could have contributed to functional reversibility and lack of retinal degeneration seen in our photo-stress model, because similar light-damage paradigm (3000 lux, 2 h) induced extensive photoreceptor death when applied to waking animals (Hafezi *et al.* 1997a). A former study showed that systemic administration of xylazine transiently induced basic fibroblast growth factor in photoreceptors but not in the brain, and this unique expression pattern contributed to photoreceptor survival following light-damage in albino rats (Wen *et al.* 1996). Despite these differences, the retina remains a delicately tunable model for studying MMP-9 induction in physiological and pathological processes, but care should be taken while extrapolating the results to the whole CNS.

Exposure of the retina to bright white light enhanced MMP-9 transcription and protein synthesis. Increased pro-MMP-9 levels on zymograms from soluble and insoluble fractions reflect gelatinase changes in both the cytosol and the extracellular space of the retina. This suggests elevated synthesis and enhanced secretion of MMP-9 after photo-stress.

Gelatin zymography detects changes in pro-enzyme and active forms of MMP-9 (Woessner 1995). Delayed increase of MMP-9 gelatinase activity (~92–100 kDa) on zymograms presumably reflects *de novo* synthesis filling up a pro-MMP-9 pool after light exposure. Besides, we cannot exclude either the transient elevation of the ~82 kDa active form of MMP-9 deteriorating rapidly and therefore hard to document on zymograms (Heo *et al.* 1999), or the possibility of the ~65 kDa lytic band to be an active MMP-9 fragment (Okada *et al.* 1992) superimposed on the rather constitutive MMP-2 (72–66 kDa). This latter hypothesis is supported by the observation that the

intensity of the ~65 kDa band increased in most samples and, that it was recognized by MMP-9 antibody on western blot (Fig. 4c).

The molecular mechanisms underlying the simultaneous and more sustained induction of pro-MMP-9 in eye structures metabolically coupled to the retina (RPE included in the 'sclera' samples, and the vitreous body) need further investigation. The successive elevation of MMP-9 mRNA in these eye structures could suggest an indirect mechanism of MMP-induction through diffusible factors originating in the photosensitive retina, similar to the paracrine induction of some MMPs described in tumor progression models (Tang *et al.* 2004). In the case of cornea, the MMP-9 elevation was partly an effect of systemic xylazine administration as shown by control experiments, and could be the basis of corneal toxicity of xylazine seen in other studies (Tita *et al.* 2001). There is a possibility of light absorbance by the transparent media of the eye to reach the level of cellular stress and initiate pro-MMP-9 induction by resident or inflammatory cells in each of these eye structures, but various optical radiation-bands are differentially absorbed by ocular media. It is well-known that UV light does not propagate past the cornea and lens, and that excessive exposure in the visible spectrum (400–700 nm) damages the retina, RPE, and choroid (Glickman 2002). As white light emitting LEDs do not emit UV light, it is hard to support the direct effect of light as the main trigger of MMP-9 induction in other tissues than the retina and the RPE. Therefore, we propose that MMP-9 induction is initiated in the retina and diffusible compounds mediate MMP induction to other tissues.

Several studies used cool fluorescent white light-induced retinal degeneration as model of apoptotic cell death (Hafezi *et al.* 1997a,b; Wenzel *et al.* 2000; Gordon *et al.* 2002). Although these studies used a wide range of light exposure paradigms they all agree in finding extensive TUNEL-positive labeling in ONL around 20 and/or 40 h and significant photoreceptor loss at 3–10 days following photo-stress. The fate of photoreceptors was shown to be the result of an intricate set of factors (earlier light-history, timing of light-exposure, drugs, a host of intrinsic features) beyond actual parameters of damaging light (intensity, wavelength, duration) (Noell *et al.* 1966; Penn *et al.* 1987). Other studies connected tissue remodeling and/or neuronal death in glutaminergic excitotoxicity models in the CNS (Gu *et al.* 2002; Rivera *et al.* 2002; Szklarczyk *et al.* 2002; Jourquin *et al.* 2003; Lee *et al.* 2004) and later in the ganglion cell layer of the retina (Zhang and Chintala 2004; Mali *et al.* 2005; Manabe *et al.* 2005) with MMP-9 induction.

In our experiments, the parameters of light, the anesthetics and the light-history of rats were adjusted so that neither extensive TUNEL-positive labeling of photoreceptor nuclei at 20 h nor significant reduction in photoreceptor cell number at 10 days after photo-stress was observed. However, minor changes in dendritic arborizations, synapse distribution, etc. cannot be excluded. Re-exposure to 500-lux room-light after a non-stressful long-lasting dark adaptation was an even milder retinal stress, obviously without retinal remodeling or cell loss. We observed MMP-9 induction in both paradigms. After photo-stress, MMP-9 induction was more intensive and widespread than after light adaptation, when it was localized to the retina. Our data show the first evidence that natural stimuli can induce MMP-9 in sensory system arguing against the idea that MMP-9 induction occurs exclusively in cell destructive models.

It is generally accepted that the ERG b-wave reflects mainly restorative ionic currents of retinal cells including a component originating in the Müller glia (Newman and Odette 1984). Although this raises the possibility of a common cellular background for reduction in b-wave amplitude and increased levels of MMP-9 seen in the retina in our photo-stress model, the elucidation of the exact cellular origin of MMP-9 needs extensive immunohistochemical analysis employing double labeling, which was beyond the scope of the present study.

In physiological conditions, ERG b-wave is extremely stable (Szabó-Salfay *et al.* 2001) and decrease in b-wave amplitude correlates with the extent of retinal damage (Sugawara *et al.* 2000). We developed the first reliable implantation method for recording ERG from freely moving rats (Galambos *et al.* 2000). We demonstrated the similarity of recorded responses to earlier ERG-descriptions (Newman and Odette 1984) and the stability of recorded signal for several weeks. It is thus a reliable method for studying functional effects of MMP-inhibitors in the retina. Application of GM6001 in DMSO decreased the rate of recovery of b-wave amplitude in comparison to DMSO-only injected control. As GM6001 is a broad-spectrum MMP-inhibitor, which binds MMP-9 with high affinity but also inhibits MMP-8, -1, -2, and -3, the involvement of these MMPs in the b-wave recovery cannot be excluded. We injected GM6001 into the retrobulbar space to avoid mechanical lesion of the eye, as traumatic injury can trigger MMP-9 induction (Wang *et al.* 2000; Planas *et al.* 2002). Retrobulbar injection is used in medical practice for enhanced drug delivery to the retina by exploiting the permeability of sclera (Raghava *et al.* 2004).

The inhibitory effect of GM6001 on functional recovery of vision after photo-stress disclosed that MMPs, particularly the inducible MMP-9, are important components of the recovery process by controlling the recovery rate. This finding supports the idea that MMP-9 induction can be restorative. The specific function of MMP-9 could be confirmed by using MMP-9 selective inhibitors or by adapting our method to MMP-9 knockout mice strains in the future. The role of MMP-9 induction in the recovery process is determined by its locally available substrates

(Larsen *et al.* 2003), but the specific substrates of MMP-9 in the retina *in vivo* are mostly unknown.

It has to be noted that DMSO by itself improved the recovery of ERGs compared to photo-stress recovery data without DMSO, in accordance with earlier studies in which DMSO was found to be excitatory, and enhancing evoked responses in the nervous system (Sawada and Sato 1975; Stolc and Vlckova 1982; McCallum 1983). Thus, our findings can be interpreted so that the DMSO effect was antagonized by MMP-9 inhibition.

Long-lasting adaptation to darkness followed by exposure to habitual room-light induced pro-MMP-9 exclusively in the Triton X-insoluble (extracellular) fraction of the retina. Re-exposure and adaptation to room-light is a gentle, non-destructive everyday experience for retinal cells and does not induce any kind of cell damage. Since a synaptic pool of MMP-9, which can efficiently tune the synaptic transmission, has been proposed (Kaczmarek *et al.* 2002; Nagy *et al.* 2006), the restricted increase in MMP-9 could indicate a physiologic role of MMP-9 in state-dependent excitability control such as light adaptation.

Our results are the first evidences of induction of MMP-9 *in vivo* by natural sensory stimuli of different intensities. The lack of significant structural and irreversible functional damage suggests a physiological role for MMP-9. Regarding further functional roles, the delayed recovery occurring after MMP-9 inhibition strongly supports the involvement of MMP-9 in retinal recovery processes after bright light exposure.

Acknowledgements

We thank Professor Miklós Palkovits and Dr Zoya Katarova for providing cryosectioning facilities, and Sarolta Pálfia and G. Milosevits for their excellent technical assistance. This work was supported by the National Science Research Grant OTKA (TS 044711, T 047217), AGYPROT, MEDICHEM II, RET, Marie Curie Reintegration Grant (IÁ), and Bolyai János Fellowship (IÁ).

References

Abu El-Asrar A. M., Dralands L., Veckeneer M., Geboes K., Missotten L., Van Aelst I. and Opdenakker G. (1998) Gelatinase B in proliferative vitreoretinal disorders. *Am. J. Ophthalmol.* **125**, 844–851.

Fini M. E., Girard M. T. and Matsubara M. (1992) Collagenolytic/gelatinolytic enzymes in corneal wound healing. *Acta Ophthalmol. Suppl.* **202**, 26–33.

Galambos R., Szabó-Salfay O., Barabás P., Pálhalmi J., Szilágyi N. and Juhász G. (2000) Temporal distribution of ganglion cell voleys in the normal rat optic nerve. *Proc. Natl Acad. Sci. USA* **97**, 13454–13459.

Glickman R. D. (2002) Phototoxicity to the retina: mechanisms of damage. *Int. J. Toxicol.* **21**, 473–490.

Gordon W. C., Casey D. M., Lukiw W. J. and Bazan N. G. (2002) DNA damage and repair in light-induced photoreceptor degeneration. *Invest. Ophthalmol. Vis. Sci.* **43**, 3511–3521.

Gu Z., Kaul M., Yan B., Kridel S. J., Cui J., Strongin A., Smith J. W., Liddington R. C. and Lipton S. A. (2002) *S*-nitrosylation of matrix metalloproteinases: signaling pathway to neuronal cell death. *Science* **297**, 1186–1190.

Gursoy-Ozdemir Y., Qiu J., Matsuoka N., Bolay H., Bermpohl D., Jin H., Wang X., Rosenberg G. A., Lo E. H. and Moskowitz M. A. (2004) Cortical spreading depression activates and upregulates MMP-9. *J. Clin. Invest.* **113**, 1447–1455.

Hafezi F., Marti A., Munz K. and Remé C. E. (1997a) Light-induced apoptosis: differential timing in the retina and pigment epithelium. *Exp. Eye Res.* **64**, 963–970.

Hafezi F., Steinbach J. P., Marti A., Munz K., Wang Z.-Q., Wagner E. F., Aguzzi A. and Remé C. E. (1997b) The absence of *c-fos* prevents light-induced apoptotic cell death of photoreceptors in retinal degeneration *in vivo*. *Nat. Med.* **3**, 346–349.

Hattori S., Fujisaki H., Kiriyama T., Yokoyama T. and Irie S. (2002) Real-time zymography and reverse zymography: a method for detection of matrix metalloproteinases and their inhibitors using FITC-labeled collagen and casein as substrates. *Anal. Biochem.* **301**, 27–34.

Heo J. H., Lucero J., Abumiya T., Koziol J. A., Copeland B. R. and Zoppo G. J. (1999) Matrix metalloproteinases increase very early during experimental focal cerebral ischemia. *J. Cereb. Blood Flow Metab.* **19**, 624–633.

Jourquin J., Tremblay E., Décanis N., Charton G., Hanessian S., Chollet A.-M., Le Dieguardher T., Khrestchatisky M. and Rivera S. (2003) Neuronal activity-dependent increase of net matrix metalloproteinase activity is associated with MMP-9 neurotoxicity after kainate. *Eur. J. Neurosci.* **18**, 1507–1517.

Kaczmarek L., Lapinska-Dzwonek J. and Szymczak S. (2002) Matrix metalloproteinases in the adult brain physiology: a link between c-Fos, AP-1 and remodeling of neuronal connections? *EMBO J.* **21**, 6643–6648.

Larsen P. H., Wells J. E., Stallcup W. B., Opdenakker G. and Yong V. W. (2003) Matrix metalloproteinase-9 facilitates remyelination in part by processing the inhibitory NG2 proteoglycan. *J. Neurosci.*, **23**, 11127–11135.

Lee S.-R., Tsuji K., Lee S.-R. and Lo E. H. (2004) Role of matrix metalloproteinases in delayed neuronal damage after transient global cerebral ischemia. *Neurobiol. Dis.* **24**, 671–678.

Mali R. S., Cheng M. and Chintala S. K. (2005) Intravitreous injection of membrane depolarization agent causes retinal degeneration via matrix metalloproteinase-9. *Invest. Ophthalmol. Vis. Sci.* **46**, 2125–2132.

Malik S., Cohen D., Meyer E. and Perlman I. (1986) Light damage in the developing retina of the albino rat: an electroretinographic study. *Invest. Ophthalmol. Vis. Sci.* **27**, 164–167.

Manabe S., Gu Z. and Lipton S. A. (2005) Activation of matrix metalloproteinase-9 via neuronal nitric oxide synthase contributes to NMDA-induced retinal ganglion cell death. *Invest. Ophthalmol. Vis. Sci.* **46**, 4747–4753.

McCallum J. E. (1983) Improvement in somatosensory evoked response amplitude and neurologic function following DMSO in a cat model of chronic spinal cord compression. *Ann. NY Acad. Sci.* **411**, 357–360.

Meighan S. E., Meighan P. C., Choudhury P., Davis C. J., Olson M. L., Zornes P. A., Wright J. W. and Harding J. W. (2006) Effects of extracellular matrix-degrading proteases matrix metalloproteinase 3 and 9 on spatial learning and synaptic plasticity. *J. Neurochem.* **96**, 1227–1241.

Nagy V., Bozdagi O., Matynia A., Balcerzyk M., Okulski P., Dzwonek J., Costa R. M., Silva A. J., Kaczmarek L. and Huntley G. W. (2006) Matrix metalloproteinase-9 is required for hippocampal late-phase long-term potentiation and memory. *J. Neurosci.* **26**, 1923–1934.

Newman E. A. and Odette L. L. (1984) Model of electroretinogram b-wave generation: a test of the K^+ hypothesis. *J. Neurophysiol.* **51**, 164–182.

Noell W. K., Walker V. S., Kang B. S. and Berman S. (1966) Retinal damage by light in rats. *Invest. Ophthalmol.* **5**, 450–473.

Okada Y., Gonoji Y., Naka K., Tomita K., Nakanishi I., Iwata K., Yamashita K. and Hayakawa T. (1992) Matrix metalloproteinase 9 (92-kDa gelatinase/Type IV collagenase) from HT 1080 human fibrosarcoma cells. Purification and activation of the precursor and enzymic properties. *J. Biol. Chem.* **267**, 21712–21719.

Penn J. S., Naash M. I. and Anderson R. E. (1987) Effect of light history on retinal antioxidant and light damage susceptibility in the rat. *Exp. Eye Res.* **44**, 779–788.

Planas A. M., Sole S. and Justicia C. (2001) Expression and activation of matrix metalloproteinase-2 and -9 in rat brain after transient focal cerebral ischemia. *Neurobiol. Dis.* **8**, 834–846.

Planas A. M., Justicia C., Sole S., Friguls B., Cervera A., Adell A. and Chamorro A. (2002) Certain forms of matrix metalloproteinase-9 accumulate in the extracellular space after microdialysis probe implantation and middle cerebral artery occlusion/reperfusion. *J. Cereb. Blood Flow Metab.* **22**, 918–925.

Raghava S., Hammond M. and Kompella U. B. (2004) Periocular routes for retinal drug delivery. *Expert Opin. Drug Deliv.* **1**, 99–114.

Rivera S., Ogier C., Jourquin J., Timsit S., Szklarczyk A. W., Miller K., Gearing A. J. H., Kaczmarek L. and Khrestchatisky M. (2002) Gelatinase B and TIMP-1 are regulated in a cell- and time-dependent manner in association with neuronal death and glial reactivity after global forebrain ischemia. *Eur. J. Neurosci.* **15**, 19–32.

Rosenberg G. A., Navratil M., Barone F. and Feuerstein G. (1996) Proteolytic cascade enzymes increase in focal cerebral ischemia in rat. *J. Cereb. Blood Flow Metab.* **16**, 360–366.

Salzmann J., Limb G. A., Khaw P. T., Gregor Z. J., Webster L., Chignell A. H. and Charteris D. G. (2000) Matrix metalloproteinases and their natural inhibitors in fibrovascular membranes of proliferative diabetic retinopathy. *Br. J. Ophthalmol.* **84**, 1091–1096.

Sawada M. and Sato M. (1975) The effect of dimethyl sulfoxide on the neuronal excitability and cholinergic transmission in Aplysia ganglion cells. *Ann. NY Acad. Sci.* **243**, 337–357.

Sivak J. M. and Fini M. E. (2002) MMPs in the eye: emerging roles for matrix metalloproteinases in ocular physiology. *Prog. Ret. Eye Res.* **21**, 1–14.

Stolc S. and Vlckova E. (1982) Facilitatory effect of some drugs on transmission in the frog sympathetic ganglion. *J. Auton. Nerv. Syst.* **6**, 335–345.

Stone J., Maslim J., Valter-Kocsi K. *et al.* (1999) Mechanisms of photoreceptor death and survival in mammalian retina. *Prog. Ret. Eye Res.* **18**, 689–735.

Sugawara T., Sieving P. A. and Bush R. A. (2000) Quantitative relationship of the photopic and scotopic ERG to photoreceptor cell loss in light damaged rats. *Exp. Eye Res.* **70**, 693–705.

Szabó-Salfay O., Pálhalmi J., Szatmári E., Barabás P., Szilágyi N. and Juhász G. (2001) The electroretinogram and visual evoked potential of freely moving rats. *Brain Res. Bull.* **56**, 7–14.

Szklarczyk A., Lapinska J., Rylski M., McKay R. D. G. and Kaczmarek L. (2002) Matrix metalloproteinase-9 undergoes expression and activation during dendritic remodeling in adult hippocampus. *J. Neurosci.* **22**, 920–930.

Taishi P., Sanchez C., Wang Y., Fang J., Harding J. W. and Krueger J. M. (2001) Conditions that affect sleep alter the expression of molecules associated with synaptic plasticity. *Am. J. Physiol. Regul. Integr. Comp. Physiol.* **281**, R839–R845.

Tang Y., Kesavan P., Nakada M. T. and Yan L. (2004) Tumor-stroma interaction: positive feedback regulation of extracellular matrix metalloproteinase inducer (EMMPRIN) expression and matrix metalloproteinase-dependent generation of soluble EMMPRIN. *Mol. Cancer Res.* **2**, 73–80.

Tita B., Leone M. G., Casini M. L. *et al.* (2001) Corneal toxicity of xylazine and clonidine, in combination with ketamine, in the rat. *Ophthalmic Res.* **33**, 345–352.

Van den Steen P. E., Dubois B., Nelissen I., Rudd P. M., Dwek R. A. and Opdenakker G. (2002) Biochemistry and molecular biology of gelatinase B or matrix metalloproteinase-9 (MMP-9). *Crit. Rev. Biochem. Mol. Biol.* **37**, 375–536.

Wang X., Jung J., Asahi M., Chwang W., Russo L., Moskowitz M. A., Dixon C. E., Fini M. E. and Lo E. H. (2000) Effects of matrix metalloproteinase-9 gene knock-out on morphological and motor outcomes after traumatic brain injury. *J. Neurosci.* **20**, 7037–7042.

Weeks J. G., Halme J. and Woessner J. F. Jr. (1976) Extraction of collagenase from the involuting rat uterus. *Biochim. Biophys. Acta* **445**, 205–214.

Wen R., Cheng T., Li Y., Cao W. and Steinberg R. H. (1996) α_2-Adrenergic agonists induce basic fibroblast growth factor expression in photoreceptors *in vivo* and ameliorate light damage. *J. Neurosci.* **16**, 5986–5992.

Wenzel A., Grimm C., Marti A., Kueng-Hitz N., Hafezi F., Niemeyer G. and Remé C. E. (2000) *c-Fos* controls the 'private pathway' of light-induced apoptosis of retinal photoreceptors. *J. Neurosci.* **20**, 81–88.

Woessner J. F. Jr. (1995) Quantification of matrix metalloproteinases in tissue samples. *Meth. Enzymol.* **248**, 510–528.

Wong T. T. L., Sethi C., Daniels J. T., Limb G. A., Murphy G. and Khaw P. T. (2002) Matrix metalloproteinases in disease and repair processes in the anterior segment. *Surv. Ophthalmol.* **47**, 239–256.

Wright J. W., Masino A. J., Reichert J. R., Turner G. D., Meighan S. E., Meighan P. C. and Harding J. W. (2003) Ethanol-induced impairment of spatial memory and brain matrix metalloproteinases. *Brain Res.* **963**, 252–261.

Young R. W. (1994) The family of sunlight-related eye diseases. *Optometry Vis. Sci.* **71**, 125–144.

Zhang X. and Chintala S. K. (2004) Influence of interleukin-1 beta induction and mitogen-activated protein kinase phosphorylation on optic nerve ligation-induced matrix metalloproteinase-9 activation in the retina. *Exp. Eye Res.* **78**, 849–860.

Zhang J. W., Deb S. and Gottshall P. E. (1998) Regional and differential expression of gelatinases in rat brain after systemic kainic acid or bicuculline administration. *Eur. J. Neurosci.*, **10**, 3358–3368.

Zhang X., Sakamoto T., Hata Y., Kubota T., Hisatomi T., Murata T., Ishibashi T. and Inomata H. (2002) Expression of matrix metalloproteinases and their inhibitors in experimental retinal ischemia-reperfusion injury in rats. *Exp. Eye Res.* **74**, 577–584.

Zhang X., Cheng M. and Chintala S. K. (2004) Kainic-acid mediated upregulation of matrix metalloproteinase-9 promotes retinal degeneration. *Invest. Ophthalmol. Vis. Sci.*, **45**, 2374–2383.

